Dopamine activation modulates oscillatory synchrony in the hippocampal-prefrontal cortex circuitry

Benedito Alves de Oliveira-Júnior[1], João Pereira Leite[1], Rafael Naime Ruggiero[1]

[1]Department of Neuroscience and Behavioral Sciences, Ribeirão Preto Medical School, University of São Paulo, Ribeirão Preto, SP 14049-900, Brazil.

Correspondence: benedito.oliveira@usp.br, rafaruggiero@usp.br

Abstract

Interaction between brain networks forms the functional unit that sustains cognition and behavior. It has been proposed that oscillatory activity can synchronize distant neuronal populations. One crucial aspect to elucidate brain function and its emergent properties is to understand how functional connectivity is modulated in different time scales according to environmental or physiological demand. Modulatory neurotransmitters such as dopamine have been implicated in changes in membrane excitability, modulation of oscillatory power, and coherence in crucial circuits for cognition, such as the hippocampus-prefrontal cortex (HPC-PFC) pathway. However, it is not known how dopaminergic release modulates specifically the phase synchrony of HPC-PFC or which specific dopaminergic receptors are responsible for the effects. In this context, our objective was to investigate the influence of dopaminergic activity on HPC-PFC synchrony and to assess whether the observed effects are receptor-specific. Our results show that dopamine induces HPC-PFC theta synchrony dose-dependently. This effect is not reproduced by apomorphine unspecific agonism or by SKF and quinpirole agonists, which act respectively on D_1- and D_2-like receptors. Additionally, we observed a late effect with peak activity between 30 and 40 minutes after dopamine 100 nmol, apomorphine 0.75 mg/kg, or quinpirole administration in which the HPC-PFC delta synchrony increased. Together, these results evidence the participation of dopaminergic neurotransmission in regulating HPC-PFC oscillatory dynamics, Influencing the synchronization in slow frequency oscillation and long-distant brain communication.

Keywords: Dopamine, oscillatory synchrony, neural connectivity, prefrontal cortex, hippocampus, ventral tegmental area, local field potential.

Introduction

The brain activity underlying animal behavior is highly flexible and distributed among neuronal networks. Neural oscillations are believed to promote the formation of neuronal ensembles and facilitate communication between ensembles from distinct brain regions (Fries, 2005; Buzsáki, 2010). Oscillations are possibly the most energy-efficient mechanism for the temporal coordination of neural activity (Buzsáki & Draguhn, 2004). Therefore, investigating how the mechanism of oscillatory synchrony works is particularly interesting to understanding the dynamic coordination of brain activity.

In a hypothesis entitled "communication through coherence", Fries (2005; 2015) proposes that coherence, a measure of synchrony, is crucial for dynamic and selective communication between brain regions. This functional communication is made possible because coherence provides a millisecond time window during which occurs the selective transfer of information between neuronal groups governed by coherent oscillations. During this period, the postsynaptic information transmission by the sender group is prioritized over other information arriving at the receiving group, ensuring selective information transfer. Fries (2015) points out that coherence is not a fixed process but rather variable and adjustable according to behavioral state and cognitive demand. In this sense, two neurophysiological processes possibly related to coherence dynamics are synaptic plasticity (Uhlhaas et al., 2010) and modulatory neurotransmission, among which dopamine stands out (Beeler & Dreyer, 2019). Two regions that exhibit dynamically coordinated activity and are mainly regulated by synaptic plasticity and modulatory neurotransmission are the hippocampus (HPC) and the prefrontal cortex (PFC; Ruggiero et al., 2021).

The HPC and PFC are anatomically connected regions widely studied for their joint role in cognitive functions and emotional processes, as well as their implication in neuropsychiatric disorders (Ruggiero et al., 2021). HPC-PFC interaction is essential for

processes such as spatial working memory and decision-making (Sigurdsson & Duvarci, 2016; Spellman et al., 2015) and is supported by hippocampal theta oscillations (Gordon, 2011; Benchenane et al., 2011). Rodent performance on spatial cognition and working memory tasks is correlated with HPC-PFC theta synchrony (Benchenane et al., 2010; Sigurdsson et al., 2010; Fujisawa & Buzsáki, 2011; O'Neill et al., 2013). Benchenane et al. (2010), using rats in a T-maze task, showed that HPC-PFC theta coherence changes dynamically during animal locomotion in the maze's central arm and peaks at the decision-making point. The increase in HPC-PFC theta coherence predicts correct choices in the maze task (Benchenane et al., 2010; Sigurdsson et al., 2010; Fujisawa & Buzsáki, 2011; O'Neill et al., 2013). Notably, Benchenane et al. (2010) also showed that HPC-PFC theta coherence increase could be reproduced by local dopamine administration in the PFC of anesthetized rats. It is known that dopamine release in the cortex increases during working memory tasks (Phillips et al., 2004). Furthermore, both agonism and antagonism of D_1- and D_2-like dopamine receptors are associated with changes in HPC-PFC theta coherence (Xu et al., 2016; Perreault et al., 2017; Gener et al., 2019), reinforcing the dopamine proposal as a neural synchrony modulator (Beeler & Dreyer, 2019).

The literature indicates that dopaminergic neurotransmission regulates the HPC-PFC oscillatory activity, mainly influencing power and coherence. (Benchenane et al., 2010; Xu et al., 2016; Perreault et al., 2017; Gener et al., 2019). However, it is not known how dopaminergic release specifically modulates HPC-PFC phase synchrony and whether the effects are receptor-specific. Considering this, we investigated the effects of dopamine administration on HPC-PFC synchrony and whether these effects are reproduced by non-specific apomorphine agonism or selective D_1- and D_2-like dopamine receptors agonism. Our findings reveal that dopamine induces HPC-PFC theta power and phase synchrony dose-dependently, and this effect is not reproduced by apomorphine or D_1- and D_2-like dopamine receptor agonism. In contrast, dopamine, apomorphine 0.75 mg/kg, and quinpirole induce late HPC-PFC delta synchrony. Therefore, our data suggest that dopaminergic neurotransmission has an essential but complex role in regulating HPC-PFC oscillatory activity, influencing not only power and coherence but also phase synchrony in slow oscillations.

Material and Methods

Animals

Forty-two male Sprague Dawley rats, seven weeks old, were used in the experiments. The animals were housed in standard rodent cages and kept in a controlled-temperature room (24 ± 2 ºC) that operated in cycles of 12 hours of light and 12 hours of dark, with lights on at 7:00 a.m. All animals had ad libitum access to food and water. This study was approved by the local ethics committee on animal experimentation (Ribeirão Preto Medical School, University of São Paulo; protocol number: 74/2021).

Experimental design

Groups are identified according to the drug administered: APO (apomorphine at concentrations of 0.75, 1.5, and 3 mg/kg); DA 500 (dopamine at a concentration of 500 nmol); DA 100 (dopamine at a concentration of 100 nmol); SKF (SKF D_1 agonist at concentrations of 1 and 10 µg); and QUIN (D_2 agonist Quinpirole at concentrations of 1 and 10 µg). Animals in each group were given a saline injection followed by a random dose of the chosen drug. The interval between injections was at least 60 minutes to avoid or reduce drug influence on the next injection.

Surgery and electrode implantation

Rats were anesthetized under urethane (1.2 mg/Kg in NaCl 0.15 M, i.p.) and placed in a stereotaxic frame (Kopf Instruments, EUA) equipped with a heating pad (Insight, Brazil) for temperature maintenance (37 ± 0.5 °C). Once the skull was exposed, burr holes were drilled, targeted at the left medial PFC (anteroposterior, AP: + 3.2 mm; medial-lateral, ML: - 0.5 mm; dorsal-ventral, DV: - 2.9 mm), the left dorsal HPC (AP: - 5.0 mm, ML: - 2.7 mm, DV: - 3.1 mm) and the right lateral ventricle (LV; AP: - 0.5 mm, ML: - 1.8 mm, DV: - 3.5 mm). Drug infusions were performed via a Hamilton microsyringe (10 µL) connected to a polyethylene tubing and a 30 gauge cannulae at a rate of 0.05 µL/min.

Stereotrodes (two 50 µm teflon-coated tungsten wires intertwined) or silicon probes (64-channel acute probe, E64+R-50-S4-L6-200 NT, ATLAS Neuroengineering, Belgium) were implanted in the PFC, and only stereotrodes were implanted in the HPC.

Stereotrodes were attached to silver wires soldered into an 8-channel connector (Omnectics Connector Corporation, EUA). Silicon probes and Omnetics connectors were coupled to 32-channel Intan headstage preamplifiers (Intan Technologies, EUA).

Extracellular recordings

The recordings were acquired using the Open Ephys acquisition system (Open Ephys Production Site, EUA). For recordings with silicon probes, the following parameters were used for signal acquisition: 1000× gain, 30 kHz sampling rate, 0.5-7603.8 Hz bandpass filtering. The parameters for recordings with tungsten wire stereotrodes were: 1000× gain , 5 kHz sample rate, 0.1-1000 Hz bandpass filtering.

Drug preparation

Apomorphine Hydrochloride (Sigma, USA), SKF-38393 Hydrochloride (Sigma, USA), and Quinpirole Hydrochloride (Sigma, USA) were directly diluted in saline (0.9% NaCl). Dopamine Hydrochloride (Sigma, USA) was diluted in 0.04 mg/ml Ascorbic Acid solution to prevent oxidation. After dilution, the drugs were preserved in a freezer at -80ºC and thawed once for use.

Brain extraction and tissue processing

At the end of the experiments, the rats anesthetized with urethane were submitted to an electrolytical lesion for histological marking of the electrode insertion sites. Rats were sacrificed with an additional dose of thiopental (25 mg/kg, i.p.). Brains were extracted and preserved in PFA (4%) over 12 hours and then in sucrose (30%) over 72 hours. Histological sections were performed in the semi-frozen brains for staining with hematoxylin and eosin and subsequent verification of the electrode insertion sites.

Data analysis

Signal analyses were performed using custom codes in MATLAB software (Mathworks, EUA). Raw LFP was downsampled to 500 Hz.

Classification of oscillatory states under urethane anesthesia

State classification was performed using the method described in Lopes-Aguiar et al. (2020). We divided the recording in 10s epochs for classification. Then we

calculated the root mean square (RMS) and the zero-crossing rate (ZC) for each epoch, which were used as input to a k-means clustering. After k-mean clustering we manually adjusted the limits of the clusters and excluded epochs that were notable outliers in order to clearly divide the epochs into tree different states: (1) Deactivated (DEA), in which the epochs exhibit slow oscillations of high amplitude and, therefore, with high RMS value and low ZC value; (2) Activated (ACT), in which predominate fast low-amplitude oscillations evidenced by a low RMS value and a high ZC value; and (3) Transition (TRANS), whose oscillatory patterns are unstable and are confused with the patterns exhibited by the other two states, with average RMS and ZC values.

Spectral power

Power spectral density (PSD) was calculated using Welch's method via the Fast Fourier Transform algorithm available in the MATLAB software. We used 3s time windows with 50% overlap and 2^{16} FFT points. We averaged the PSD estimates across trials and animals, respectively. For statistics, we integrate the powers into specific frequency bands (delta: 0.5-2 Hz, low theta: 3-6 Hz, high theta: 6-10 Hz, low gamma: 30-55 Hz). We calculate the relative power by dividing the PSD estimate by the integrated power over the frequency range of 0.5-55 Hz. For spectrograms of the whole recording, we used the mtspecgramc function from Chronux toolbox (Bokil et al., 2010), using the multi-tapered window method (5 tapers of 3s).

Functional connectivity

Spectral coherence, pairwise phase consistency (PPC; Vinck et al., 2010) and debiased weighted phase lag index (DWPLI; Vinck et al., 2011) measures were estimated using cross PSDs of HPC and PFC calculated using modified Welch's periodogram method. Spectral coherence is the same as that obtained by MATLAB's mscohere function and indicates how well the signals being compared match each other at each frequency. PPC is calculated as described by Vinck et al. (2010) and indicates unbiasedly how similar the relative oscillation phase is between trials. The DWPLI is calculated as described by Vinck et al. (2011) and indicates the phase relationship between the oscillations without interference from volume conduction bias.

For coherograms of the whole recording, we used the cohgramc function from Chronux toolbox (Bokil et al., 2010) with multi-tapered window method and the same parameters described for spectrograms.

Statistical Analysis

We evaluated the residuals, homoscedasticity, probability distribution plots (QQ plots), and the Shapiro-Wilk normality test to verify the data distribution. To compare two experimental groups, we used the paired or unpaired two-tailed Student's T test, or the non-parametric tests Wilcoxon matched-pairs signed rank test or the Mann-Whitney test, respectively. For comparing more than two experimental groups, we used one-way or two-way ANOVA with repeated measures and multiple comparisons with P-value corrected by Tukey's or Bonferroni's post-hoc test. As an alternative to ANOVA, due to the presence of missing values, we used the linear mixed effects model (LMM) with repeated measures and multiple comparisons with p-value corrected by Dunnett's post-hoc test. All statistical analyzes were performed using the GraphPad Prism 9.0 software (GraphPad Software, EUA).

Results

Initially, to evaluate the effects generated by manipulation of dopaminergic receptors on HPC-PFC activity, we performed systemic administration (i.p.) of three different apomorphine doses (0.75, 1.5, and 3 mg/kg) chosen because they are the most frequently used in the literature to produce behavioral effects. We performed the analyzes at three levels, namely: (1) the influence of the drug on the dynamics of the oscillatory states characteristic of urethane anesthesia; (2) the drug's influence on the spectral properties of electrophysiological activity; and (3) the drug's influence on HPC-PFC connectivity.

Dose-dependent changes in the dynamics of oscillatory states after APO administration

APO had a dose-dependent effect on the time proportion of states. The low dose administration (0.75 mg/kg) increased the time proportion of DEA states (t test, $t(3)=5.418$, $p=0.012$; Fig. 2A) while reduced in TRANS states (t test, $t(3)=3.184$, $p=0.049$; Fig. 2A). Similarly, the intermediate dose (1.5 mg/kg) decreased the time

proportion of TRANS states (t test, t(5)= 3.636, p=0.015; Fig 2A). In contrast, the high dose (3 mg/kg) increase time proportion of ACT states (t test, t(4)=3.400, p=0.027; Fig. 2A). In addition, we also evaluated the average time proportion of states, which indicates whether a change in the duration of a state is consistent across occurrences of the respective state. We observed an increase in the average time proportion of DEA states after APO 0.75 mg/kg administration (t test, t(3)=2.872, p=0.063; Fig. 2B) and ACT states after APO 3 mg/kg administration (t test, t(4)=2.565, p=0.062; Fig. 2B). Taken together, these results demonstrate that apomorphine induces a predominance of DEA states at a low dose, and at a high dose, it induces a predominance of ACT states.

Spectral and connectivity changes after APO administration

The spectral activity is also affected in a dose-dependent manner, which is verified by the coherence and power spectrograms, and by the theta/delta ratio (Fig. 3). To investigate whether APO influences HPC-PFC synchrony, we evaluated the spectral coherence of different frequency bands over time to determine the peak effect (Fig. 3E), and performed the PSD of the spectral coherence, comparing the baseline with the period of effect after injection (Fig. 4). Spectral coherence is one of the primary measures used to assess synchrony between two brain regions. However, this measure is considerably dependent on and biased by spectral power. As observed in the literature (Benchenane et al., 2010), an increase in HPC-PFC coherence may occur without necessarily observing an increase in power. In this sense, we also decided to use two phase synchrony measures that are less biased by spectral power, the PPC (Vinck et al., 2010) and the DWPLI (Vinck et al., 2011). We observed that apomorphine 0.75 mg dose shifts brain oscillation to a delta prominent state. There is a reduction in theta/delta ratio and high theta relative power, and an increase in delta coherence. This high theta increase is significant in HPC (t test, t(3)=4.305, p=0.023; Fig. 4A), which presents also an increase in delta relative power (t test, t(3)=2.469, p=0.090; Fig. 4A). Despite the increase in delta coherence (t test, t(3)=3.004, p=0.057; Fig. 4B), there is no other effect on HPC-PFC synchrony. Differently, in the APO 1.5 mg/kg group there were no statistical differences (Fig. 4C,D). Finally, the APO 3 mg/kg dose has the opposite effect of the low dose, inducing an theta prominent state. There

is a gradual increase in the theta/delta ratio over time and an increase in low theta relative power accompanied by a decrease in delta coherence. Effects in relative power occur at both PFC (delta: t test, $t(4)=3.363$, $p=0.028$; low theta: t test, $t(4)=2.166$, $p=0.096$; Fig. 4E) and HPC (delta: t test, $t(4)=2.953$, $p=0.041$; low theta: t test, $t(4)=2.357$, $p=0.077$; Fig. 4E). Furthermore, the reduction in delta coherence (t test, $t(4)=3.026$, $p=0.038$; Fig. 4F) is accompanied by a non-significant reduction in high theta coherence (t test, $t(4)=2.162$, $p=0.096$; Fig. 4F).

APO dose-dependent effects on slow oscillations are also partially seen in low gamma oscillations (Fig. 5). APO 0.75 mg/kg, but not higher doses, increases low gamma coherence (t test, $t(3)=4.411$, $p=0.021$; Fig. 5C) without significantly affecting relative power or other measures of synchrony. APO 3 mg/kg, but not lower doses, increases low gamma relative power without affecting synchrony. This increase in relative power occurs in both PFC (Wilcoxon, $W=15$, $p=0.062$; Fig 5F) and HPC (Wilcoxon, $W=15$, $p=0.062$; Fig. 5G). Interestingly, APO 0.75 mg/kg induces a gradual increase in coherence over time, which does not occur at other doses (Fig. 5A). Finally, another differential effect between APO doses is the change in the PSD slope. While APO 0.75 mg/kg administration produced an increase in the PSD slope, APO 1.5 mg/kg e 3 mg/kg groups showed a decrease in this slope (Fig. 5B,D,F)

These data show that APO administration have opposite effects on oscillations according to the dose used. Low doses produce a delta prominent state, while higher doses increase theta oscillations predominance.

Changes in the dynamics of oscillatory states after DA administration

In order to more selectively investigate the effects of dopaminergic neurotransmission, we administered DA 500 nmol or DA 100 nmol doses. DA 500 nmol group showed an increase in the time proportion of TRANS states (t test, $t(12)=2.735$, $p=0.018$; Fig. 6B). In contrast, the 100 nmol DA group exhibited a prevalence of DEA states, with both higher time proportion (t test, $t(7)=6.305$, $p<0.001$; Fig. 6A) and higher average time proportion (t test, $t(7)=2.392$, $p=0.048$; Fig. 6B) of DEA states. This effect was accompanied by the reduction in time proportion of ACT states (t test,

t(7)=3.843, p=0.006; Fig. 6A). These results demonstrate that DA induces a predominance of DEA states at a low dose but less clear changes at a high dose.

Spectral and connectivity changes after DA administration

We observed that both DA doses induce changes in coherence and power, as well as in theta/delta ratio, especially in the initial 20 minutes after injection (Figs. 7A-B and 9A-B). Interestingly, despite the increase in DEA state, DA 100 nmol initially induces a decrease in delta oscillations. Both delta coherence and HPC delta relative power were reduced (HPC delta: t test, t(7)=2.735, p=0.029; delta coherence: t test, t(7)=2.839 p=0.025; Fig. 8A,B). DA 500 nmol produced similar but more robust effects, resulting in delta suppression and theta predominance. Specifically, DA 500 nmol induced a general reduction in delta relative power (PFC: t test, t(12)=3.550, p=0.004; HPC: t test, t(12)=3.846, p=0.002; Fig. 10A) accompanied by a general increase in theta relative power (PFC – low theta: t test, t(12)=3.413, p=0.005; PFC – high theta: t test, t(12)=2.805, p=0.015; HPC – low theta: t test, t(12)=3.969, p=0.001; HPC – high theta: t test, t(12)=2.743, p=0.017; Fig. 10A). Despite the robust effects in theta relative power, DA 500 nmol does not affects low theta coherence but reduces delta coherence (t test, t(12)=3.098, p=0.009; Fig. 10B) and increases high theta coherence (t test, t(12)=2.682, p=0.019; Fig. 10B). The increase in HPC-PFC connectivity promoted by DA 500 nmol also includes an increase in theta PPC and theta DWPLI (PPC – low theta: t test, t(12)=3.212, p=0.007; PPC – high theta: t test, t(12)=3.582, p=0.003; DWPLI – low theta: t test, t(12)=3.238, p=0.007; DWPLI – high theta: t test, t(12)=3.852, p=0.002; Fig. 10B). These results indicate that higher dopamine doses induce increased theta power and synchrony, promoting HPC-PFC connectivity without bias by power or dependence on volume conduction.

Interestingly, both DA doses exhibited a late effect, which peaks around 30 to 40 minutes after injection. While DA 500 nmol produced more robust effects in the initial post-injection period, DA 100 nmol resulted in more expressive effects in the late period. During this late effect, the DA 100 nmol group showed an increase in HPC delta relative power (t test, t(7)=3.535, p=0.009; Fig. 8C) and a decrease in theta relative power in the same region (low theta: t test, t(7)=4.403,p=0.003; high theta: t test, t(7)=2.433, p=0.045; Fig. 8C). There was also an increase in delta coherence (t test,

t(7)=2.153, p=0.068; Fig. 8D) and a reduction in high theta coherence (t test, e agt(7)=2.144, p=0.069; Fig. 8D), but no change in phase synchrony. Notably, most of these effects are opposite to those observed in the initial period after administration of the same dose. This pattern was also observed in the DA 500 nmol group, with no effects on relative power, but it was observed a reduced high theta coherence (Wilcoxon, W=-87, p<0.001; Fig. 10D). This effect contrasts with the increase in high theta phase coherence and synchrony observed in the initial post-injection period. In general, the oscillatory changes in the initial and late period demonstrate that the effects resulting from the administration of DA are manifested not only dose-dependently but also in a time-dependent way.

Absence of effects on the dynamics of oscillatory states after administration of dopamine agonists SKF (D_1) and QUIN (D_2)

To investigate whether the effects observed by DA administration are receptor-specific, we administered the selective D_1 receptor agonist, SKF, and the D_2 receptor agonist, QUIN. We found that both SKF and QUIN agonists, regardless of dose, do not promote changes in the time proportion of oscillatory states (Fig. S1A-D) and therefore do not reproduce the effects exhibited by dopamine on the dynamics of urethane oscillatory states.

Absence of spectral and connectivity changes after SKF administration

We observed that both doses of SKF (1 and 10 µg) did not produce evident changes in spectrograms or in theta/delta ratio relative power (Fig. S2). However, SKF 10 µg produced a trend towards reduced low theta coherence (t test, t(5)=2.352, p=0.065; Fig. S3D), which is the opposite effect of the higher dose of dopamine administration. No other effects on synchrony were observed. The almost total absence of effects may possibly indicate that the selected D_1 agonist doses are insufficient to reproduce a physiological activation of D_1 receptors.

Spectral and connectivity changes after QUIN administration

We found that both doses of QUIN (1 µg and 10 µg) induced visible changes in spectrograms and in theta/delta ratio relative power (Fig. 11). Although there were no effects in the initial post-injection period, QUIN shifts oscillations to a delta prominent

state in the late period. In HPC, QUIN 1 µg resulted in an increase in delta relative power (t test, t(5)=2.966, p=0.031; Fig. 12E) and a low theta relative power reduction (t test, t(5)=3.299, p=0.021; Fig 12E). These effects were accompanied by a reduction in PFC theta relative power (Wilcoxon, W=-21, p=0.031; Fig. 12E) and a reduction in high theta coherence (t test, t(5)=3.169, p=0.024; Fig. 12F). Furthermore, we verified an increase in delta coherence (t test, t(5)=3.960, p=0.010; Fig. 12F), which was also observed after APO 0.75 mg/kg and DA 100 nmol administration, the two lowest doses of the respective drugs. Given that APO operates on D_1 and D_2 receptors, and DA may have more affinity for D_2 receptors than D_1 (Marcellino et al., 2011), D_2 receptor agonism may be especially associated with increased delta activity. Interestingly, the highest dose of QUIN had similar but more robust effects to the lower dose. In both HPC and PFC, QUIN 10 µg resulted in an increase in delta relative power (PFC: t test, t(5)=2.634, p=0.046; HPC: t test, t(5)=2.678, p=0.043; Fig. 12G) and a decrease in low theta relative power (PFC: t test, t(5)=3.035, p=0.028; HPC: t test, t(5)=2.775, p=0.039; Fig. 12G). We also found that a general increase in delta synchrony accompanied these effects. Specifically, there was an increase in delta coherence (t test, t(5)=5.814, p=0.002; Fig. 12H) and delta phase synchrony (PPC – t test, t(5)=3.054, p=0.028; DWPLI – t test, t(5)=3.263, p=0.022; Fig. 12H). Finally, there was an increase in low theta coherence (t test, t(5)=4.166, p=0.008; Fig. 12H). Taken together, these results demonstrate that QUIN activation of dopaminergic D_2 receptors results in late oscillatory and dose-dependent changes, among which the increase in delta power and connectivity stands out.

Drugs	**Power**						**Coherence**				**PPC**			**DWPLI**	
	Delta		Low theta		High theta		Delta	Low theta	High theta	Delta	Low theta	High theta	Delta	Low theta	High theta
	PFC	HPC	PFC	HPC	PFC	HPC	HPC-PFC	HPC-PFC	HPC-PFC	HPC-PFC	HPC-PFC	HPC-PFC	HPC-PFC	HPC-PFC	HPC-PFC
APO 0.75 mg/kg		↗		↘		↓	↗								
APO 1.5 mg/kg															
APO 3 mg/kg	↓	↓	↗	↗			↓		↘						

DA 100 nmol	↗	↓ ↑	↘	↓	↓	↗	↓ ↗		↘					
DA 500 nmol	↓	↓	↑	↑	↑	↑	↓		↑ ↓		↑	↑	↑	↑
SKF 1 µg														
SKF 10 µg								↘						
QUIN 1 µg		↑		↓	↘		↑	↘ ↘	↓					
QUIN 10 µg	↑	↑	↓	↓	↘		↑	↓		↑		↑		

Table 1. Summary of main oscillatory changes in initial (blue) or late (red) periods after drug injections. Legend: ↑, increase, $p<0.05$; ↓, reduction, $p<0.05$; ↗, increase trend, $p<0.1$; ↘, reduction trend, $p<0.1$.

Discussion

In this study, we investigated the specific effects of selective and non-selective agonism of D_1 and D_2 dopamine receptors and the exogenous DA effects on HPC-PFC oscillatory dynamics. Our results show that DA modulates brain dynamics inducing theta oscillations in HPC-PFC circuits. In a higher dose, DA increases theta relative power, as well as theta phase synchrony and coherence. These oscillatory changes are distinct from the nonspecific agonist apomorphine, which in low dose shifts brain oscillation to a delta prominent state, increasing delta relative power and coherence. In higher dose induces a theta state, reducing delta relative power and coherence and increasing theta relative power. Furthermore, selective agonism of D_1 or D_2 dopamine receptors did not reproduce the effects of DA on the brain, however, D_2 agonism produced a delta prominent state in the late period after injection, increasing delta relative power, as well as delta phase synchrony and coherence.

Effects on oscillatory brain state

Urethane anesthesia produces oscillatory states that spontaneously alternate between activated (ACT) and deactivated (DEA) periods and whose activity patterns are similar to those presented in natural sleep states (Clement et al., 2008). During ACT states, rapid low-amplitude oscillations and an HPC to PFC 4 Hz synchronization predominate. In DEA states, there are high amplitude slow oscillations and a PFC to

HPC 1 Hz synchronization predominance (Lopes-Aguiar et al., 2020). Experimental studies have shown that sleep and wakefulness (Oishi & Lazarus, 2017) and urethane anesthesia are both regulated by D_1- and D_2-like dopaminergic receptors (Monti & Jantos, 2008). Our results reveal that dopamine and nonspecific agonist apomorphine, but not the selective D_1 and D_2 agonists, induce dose-dependent changes in urethane oscillatory states.

We show that nonspecific D_1/D_2 APO agonism has a dose-dependent effect on HPC-PFC oscillatory dynamics. Actually, APO is known to produce biphasic effects on sleep-wake regulation. While a low dose produces sedative effects and increases the slow oscillations (Kropf & Kuschinsky, 1991, Monti & Jantos, 2008; Xu et al., 2011), high doses promote the opposite effect (Monti & Jantos, 2008). Our data confirm this biphasic APO pattern. While a low APO dose induced DEA states predominance, delta activity increase, and theta reduction, a high dose promoted ACT states predominance, delta activity reduction, and theta increase. The intermediate APO dose induced a theta oscillation peak in the PSD without statistical effect, indicating a possible weaker or more variable effect. This biphasic APO effect possibly occurs because low agonist doses act on dopaminergic neurons' autoreceptors, inhibiting these neurons and decreasing DA release, while high doses stimulate postsynaptic receptors, releasing DA directly (Skirboll et al., 1979; Monti & Jantos, 2008). Additionally, low APO doses reduce dopaminergic firing rate (Bunney et al., 1973; Mallet et al., 2008; Assié et al., 2009; Xu et al., 2011), while higher doses can promote neuronal excitability (Yanagihashi et al., 1991).

Our results indicate that higher APO doses possibly induce a hyperdopaminergic state characterized by an increase in HPC and PFC low gamma relative power. It is well established that similar APO doses induce behavioral stereotypy and hyperlocomotion (Geyer et al., 1986). Both gamma band power aberrant changes (Lee et al., 2003) and behavioral stereotypy, in addition to the psychosis symptom, are characteristic of schizophrenia pathology, which according to the dopaminergic hypothesis of schizophrenia, is associated with hyperdopaminergic states. (Meltzer & Stahl, 1976). Interestingly, unlike drugs such as amphetamines, which at high doses reproduce schizophrenia symptoms by increasing the synaptic DA

availability, it is unclear whether hyperdopaminergia generated by high APO doses precisely reproduces the psychosis symptom (Dépatie & Lal, 2000). A possible explanation is that APO acts directly on postsynaptic dopaminergic receptors, showing a higher affinity for D_2 receptors and a lower affinity for D_3 receptors than the DA molecule (Dépatie & Lal, 2000). This would explain why APO partially reproduces schizophrenia symptoms compared to drugs releasing DA into synapses and helps to explain the differences between APO and DA in HPC-PFC oscillatory dynamics shown in our results.

Our results show that DA administration promotes dose- and time-dependent changes in HPC-PFC oscillatory dynamics. In the initial post-injection period, both DA 100 nmol and 500 nmol doses induced theta oscillations and ACT states predominance for at least 10 continuous minutes, but DA 500 nmol effects were more expressive and permanent, showing higher theta synchrony. These results confirm previous studies (Benchenane et al., 2010), indicating active DA participation in HPC-PFC oscillatory states regulation and sleep-wake systems (Oishi & Lazarus, 2017; Monti & Jantos, 2008). Interestingly, it was shown that acute dopamine depletion suppresses REM sleep and that hyperdopaminergia generated by D_2 agonist administration was necessary, but possibly not sufficient by itself, to restore REM-like oscillations (Dzirasa et al., 2006). This result indicates that the regulation of oscillatory states may depend on the dopamine interaction with other neurotransmitter systems, such as the cholinergic system (Lester et al., 2010; Monti & Jantos, 2008). Indeed, cholinergic agonists can produce ACT states, while cholinergic antagonists produce prolonged DEA states (Clement et al., 2008, Schall & Dickson, 2009). These results suggest that dopaminergic and cholinergic systems may interact in maintaining urethane states and the sleep-wake system (Dzirasa et al., 2006, Monti & Jantos, 2008).

In the late post-DA injection period, changes in oscillatory dynamics are precisely opposite to those in the initial period. DA 100 nmol dose induced theta oscillations reduction and delta oscillations predominance. DA 500 nmol dose did not produce the same effect but induced a reduction in high theta coherence. One explanation for this late phenomenon of oscillatory dynamics changing involves an alternative cell signaling cascade induced only by D_2 receptors (Dimpfel, 2008).

Although D_1 and D_2 receptor's cellular signaling pathway is traditionally known to involve G-proteins and cAMP-PKS pathways, DA can act via cAMP-independent mechanisms, such as β-arrestin proteins, which allow the desensitization of G-protein-coupled receptors (Beaulieu et al., 2005). The effect generated is an increase in delta activity beginning approximately 30 minutes after D_2 dopamine receptor agonists or exogenous DA administration (Dimpfel, 2008). This evidence explains the late effect observed in our results.

HPC-PFC oscillatory synchrony

One of our study's main results was that DA could induce HPC-PFC theta synchrony. Consistent with our result, Benchenane et al. (2010) showed that DA infused into the PFC of anesthetized rats could induce HPC-PFC theta coherence and reorganize PFC neurons firing rate into theta. However, this result was demonstrated with a low sample of animals, requiring further experimental confirmation with an adequate number of animals. Furthermore, to assess HPC-PFC synchrony, Benchenane et al. (2010) used only spectral coherence, which is highly dependent on spectral power and, therefore, possibly biased. Notably, Benchenane et al. (2010) note that despite the coherence increase, there is no power change in both HPC and PFC, indicating that DA increased phase synchrony. Using synchrony measures independent of power we showed that the increase in HPC-PFC theta phase synchrony occurs robustly in many animals following DA administration. Interestingly, Xu et al. (2016) showed in anesthetized rats that a reduction in HPC-PFC theta phase synchrony and theta power could be induced after D_1 receptor antagonist administration. In contrast, D_1 receptor agonist systemic administration increased theta coherence in pharmacological animal models of schizophrenia but not in control animals (Perreault et al., 2017). Despite these effects observed in literature, our results do not indicate D_1 receptor agonism participation in HPC-PFC synchrony, indicating that the dose used was insufficient to mimic DA activity. Indeed, the doses used in the studies described (Xu et al., 2016; Perreault et al., 2017) were at least 10 times higher than the highest dose used in our study. In another study, a reduction in HPC-PFC theta phase synchrony was observed in freely-moving animals after D_2 receptor agonist or antagonist infusion (Gener et al., 2019). Furthermore, D_2 receptor agonism, but not

antagonism, increased delta phase synchrony (Gener et al., 2019). These effects are similar to the late effect of D_2 agonism observed in our study. In fact, the results presented by Gener et al. (2019) refer to the period between 25 and 35 minutes after D_2 agonist or antagonist administration, indicating that the observed effect may be a late phenomenon resulting from the alternative mechanism of D_2 receptors functioning described previously. Finally, despite this set of studies showing dopaminergic participation in HPC-PFC coherence and phase synchrony, it is not possible to state whether the effects being measured in these studies would not be a reflection of electrical currents conducted by volume from HPC to cortex (Sirota et al., 2008). Our results using DWPLI (Vinck et al., 2011), a phase synchrony measure unbiased by volume conduction, indicate that the HPC-PFC phase synchrony observed is independent of volume conduction.

Oscillatory synchrony is proposed as the most efficient mechanism for neuronal activity temporal coordination (Buzsáki & Draguhn, 2004) and is essential for information transfer between distant brain regions (Varela et al., 2001; Harris & Gordon, 2015), being the main functional connectivity measure between brain regions (Gordon, 2011). It is proposed that synchrony between neuronal groups, measured as coherence between oscillations, establishes the necessary conditions for selective and effective information transfer between brain regions (Fries, 2005; 2015). In contrast, it is also proposed that this synchrony derives from the structural connectivity between neuronal groups and would therefore be a consequence, not the cause, of the functional connectivity (Schneider et al., 2021). However, both proposals for synchrony as a cause or consequence of functional connectivity are consistent with the fact that synchrony is not a fixed process but rather dynamic and modulable. In this sense, our results provide evidence that dynamic control of synchrony between distant regions may directly involve dopaminergic participation. Indeed, it has been shown in rodents that HPC-PFC theta synchrony increase can occur during new environments exploration (Siapas et al., 2005; Sirota et al., 2008; Dzirasa et al., 2009), exposure to anxiogenic stimuli (Adhikari et al., 2010) and performing cognitive tasks involving decision making and working memory (Jones & Wilson, 2005; Sigurdsson et al., 2010; Benchenane et al., 2010; Hyman et al., 2010; O'Neill et al., 2013). In cognitive tasks,

synchrony has been shown to change as a function of performance (Hyman et al., 2010; Benchenane et al., 2010; Sigurdsson et al., 2010, O'Neill et al., 2013) and peak at decision-making moments after learning the task rules (Benchenane et al., 2010). This HPC-PFC theta synchrony at decision-making choice is reproduced by infusing physiological amounts of exogenous DA into PFC (Benchenane et al., 2010). Notably, under conditions of genetic hyperdopaminergia, impairment in spatial cognitive performance is observed (Dzirasa et al., 2009; Duvarci et al., 2018). Taken together, these studies suggest that HPC-PFC theta synchrony is dynamically adjusted as a function of cognitive demand, and this adjustment may be dependent on dopaminergic action. Consistent with this claim, our results indicate that DA induces an increase in HPC-PFC theta synchrony in a dose-dependent manner, suggesting that DA can promote this dynamic adjustment of synchrony.

One of our study's main limitations is that our results were observed in anesthetized animals. It is known that urethane anesthesia has well-defined oscillatory states, and oscillatory brain patterns in anesthetized animals differ extensively from those observed in awake animals. Thus, additional experiments with freely-moving animals are necessary to generalize the results observed in this study. Furthermore, future studies should address how the precise spatiotemporal control of dopaminergic neurons in the ventral tegmental area, the main source of mesocortical dopamine, modulates the HPC-PFC oscillatory dynamics; how different patterns of dopaminergic release differentially affect HPC-PFC connectivity; and whether dopamine projected from different regions has similar regulatory effects.

Conclusion

Our study provides evidence that HPC-PFC oscillatory states under urethane anesthesia are dose- and time-dependently modulated by dopamine, as well as by the nonspecific apomorphine agonism and the specific D_2 receptor agonism. We also showed that dopamine modulates brain dynamics inducing theta oscillation and theta synchrony in HPC-PFC circuits. Our experimental evidence contributes to a better understanding of the dopaminergic role in oscillatory dynamics coordination and the consequent facilitation of HPC-PFC interaction.

Acknowledgments

This research was funded by the Coordination for the Improvement of Higher Education Personnel (B.A.O.J.: 88887.469138/2019-00) and the São Paulo Research Foundation (R.N.R.: 2018/02303-4; J.P.L.: 2016/17882-4). We thank Antonio Renato Meirelles e Silva, Renata Caldo Scandiuzzi and Daniela Ribeiro for their technical support, and Tamiris Prizon, José Luiz Liberato and Leonardo Rakauskas Zacharias for their experimental support. RNR and BAOJ designed the research. BAOJ conducted the experiments. BAOJ and RNR analyzed data. RNR and JPL supervised the project. All authors wrote and revised the manuscript.

Conflict of interest

The authors declare no competing financial interests.

References

Adhikari, A., Topiwala, M. A., & Gordon, J. A. (2010). Synchronized activity between the ventral hippocampus and the medial prefrontal cortex during anxiety. Neuron, 65(2), 257-269.

Assié, M. B., Mnie-Filali, O., Ravailhe, V., Benas, C., Marien, M., Bétry, C., ... & Newman-Tancredi, A. (2009). F15063, a potential antipsychotic with dopamine D2/D3 receptor antagonist, 5-HT1A receptor agonist and dopamine D4 receptor partial agonist properties: influence on neuronal firing and neurotransmitter release. European journal of pharmacology, 607(1-3), 74-83.

Beaulieu, J. M., Sotnikova, T. D., Marion, S., Lefkowitz, R. J., Gainetdinov, R. R., & Caron, M. G. (2005). An Akt/β-arrestin 2/PP2A signaling complex mediates dopaminergic neurotransmission and behavior. Cell, 122(2), 261-273.

Beeler, J. A., & Dreyer, J. K. (2019). Synchronicity: the role of midbrain dopamine in whole-brain coordination. Eneuro, 6(2).

Benchenane, K., Peyrache, A., Khamassi, M., Tierney, P. L., Gioanni, Y., Battaglia, F. P., & Wiener, S. I. (2010). Coherent theta oscillations and reorganization of spike timing in the hippocampal-prefrontal network upon learning. Neuron, 66(6), 921-936.

Benchenane, K., Tiesinga, P. H., & Battaglia, F. P. (2011). Oscillations in the prefrontal cortex: a gateway to memory and attention. Current opinion in neurobiology, 21(3), 475-485.

Bunney, B. S., Aghajanian, G. K., & Roth, R. H. (1973). Comparison of effects of L-dopa, amphetamine and apomorphine on firing rate of rat dopaminergic neurones. Nature New Biology, 245(143), 123-125.

Buzsáki, G. (2010). Neural syntax: cell assemblies, synapsembles, and readers. Neuron, 68(3), 362-385.

Buzsáki, G., & Draguhn, A. (2004). Neuronal oscillations in cortical networks. Science, 304(5679), 1926-1929.

Clement, E. A., Richard, A., Thwaites, M., Ailon, J., Peters, S., & Dickson, C. T. (2008). Cyclic and sleep-like spontaneous alternations of brain state under urethane anaesthesia. PloS one, 3(4), e2004.

Colgin, L. L. (2011). Oscillations and hippocampal–prefrontal synchrony. Current opinion in neurobiology, 21(3), 467-474.

Dépatie, L., & Lal, S. (2001). Apomorphine and the dopamine hypothesis of schizophrenia: a dilemma?. Journal of Psychiatry and Neuroscience, 26(3), 203.

Dimpfel, W. (2008). Pharmacological modulation of dopaminergic brain activity and its reflection in spectral frequencies of the rat electropharmacogram. Neuropsychobiology, 58(3-4), 178-186.

Duvarci, S., Simpson, E. H., Schneider, G., Kandel, E. R., Roeper, J., & Sigurdsson, T. (2018). Impaired recruitment of dopamine neurons during working memory in mice with striatal D2 receptor overexpression. Nature Communications, 9(1), 1-13.

Dzirasa, K., Ribeiro, S., Costa, R., Santos, L. M., Lin, S. C., Grosmark, A., ... & Nicolelis, M. A. (2006). Dopaminergic control of sleep–wake states. Journal of Neuroscience, 26(41), 10577-10589.

Dzirasa, K., Ramsey, A. J., Takahashi, D. Y., Stapleton, J., Potes, J. M., Williams, J. K., ... & Nicolelis, M. A. (2009). Hyperdopaminergia and NMDA receptor hypofunction disrupt neural phase signaling. Journal of Neuroscience, 29(25), 8215-8224.

Fries, P. (2005). A mechanism for cognitive dynamics: neuronal communication through neuronal coherence. Trends in cognitive sciences, 9(10), 474-480.

Fries, P. (2015). Rhythms for cognition: communication through coherence. Neuron, 88(1), 220-235.

Fujisawa, S., & Buzsáki, G. (2011). A 4 Hz oscillation adaptively synchronizes prefrontal, ATV, and hippocampal activities. Neuron, 72(1), 153-165.

Gener, T., Campo, A. T., Alemany-González, M., Nebot, P., Delgado-Sallent, C., Chanovas, J., & Puig, M. V. (2019). Serotonin 5-HT1A, 5-HT2A and dopamine D2 receptors strongly influence prefronto-hippocampal neural networks in alert mice: Contribution to the actions of risperidone. Neuropharmacology, 158, 107743.

Geyer, M. A., Russo, P. V., Segal, D. S., & Kuczenski, R. (1987). Effects of apomorphine and amphetamine on patterns of locomotor and investigatory behavior in rats. Pharmacology Biochemistry and Behavior, 28(3), 393-399.

Gordon J. A. (2011). Oscillations and hippocampal-prefrontal synchrony. Current opinion in neurobiology, 21(3), 486–491. https://doi.org/10.1016/j.conb.2011.02.012

Harris, A. Z., & Gordon, J. A. (2015). Long-range neural synchrony in behavior. Annual review of neuroscience, 38, 171-194.

Hyman, J. M., Zilli, E. A., Paley, A. M., & Hasselmo, M. E. (2010). Working memory performance correlates with prefrontal-hippocampal theta interactions but not with prefrontal neuron firing rates. Frontiers in integrative neuroscience, 2.

Jones, M. W., & Wilson, M. A. (2005). Theta rhythms coordinate hippocampal–prefrontal interactions in a spatial memory task. PLoS biology, 3(12), e402.

Kropf, W., & Kuschinsky, K. (1991). Electroencephalographic correlates of the sedative effects of dopamine agonists presumably acting on autoreceptors. Neuropharmacology, 30(9), 953-960.

Lee, K. H., Williams, L. M., Breakspear, M., & Gordon, E. (2003). Synchronous gamma activity: a review and contribution to an integrative neuroscience model of schizophrenia. Brain Research Reviews, 41(1), 57-78.

Lester, D. B., Rogers, T. D., & Blaha, C. D. (2010). Acetylcholine–dopamine interactions in the pathophysiology and treatment of CNS disorders. CNS neuroscience & therapeutics, 16(3), 137-162.

Lopes-Aguiar, C., Ruggiero, R. N., Rossignoli, M. T., Esteves, I. D. M., Peixoto-Santos, J. E., Romcy-Pereira, R. N., & Leite, J. P. (2020). Long-term potentiation prevents ketamine-induced aberrant neurophysiological dynamics in the hippocampus-prefrontal cortex pathway in vivo. Scientific reports, 10(1), 1-15.

Mallet, N., Pogosyan, A., Sharott, A., Csicsvari, J., Bolam, J. P., Brown, P., & Magill, P. J. (2008). Disrupted dopamine transmission and the emergence of exaggerated beta oscillations in subthalamic nucleus and cerebral cortex. Journal of Neuroscience, 28(18), 4795-4806.

Marcellino, D., Kehr, J., Agnati, L. F., & Fuxe, K. (2012). Increased affinity of dopamine for D2-like versus D1-like receptors. Relevance for volume transmission in interpreting PET findings. Synapse, 66(3), 196-203.

Meltzer, H. Y., & Stahl, S. M. (1976). The dopamine hypothesis of schizophrenia: a review. Schizophrenia bulletin, 2(1), 19.

Monti, J. M., & Jantos, H. (2008). The roles of dopamine and serotonin, and of their receptors, in regulating sleep and waking. Progress in brain research, 172, 625-646.

O'Neill, P. K., Gordon, J. A., & Sigurdsson, T. (2013). Theta oscillations in the medial prefrontal cortex are modulated by spatial working memory and synchronize with the hippocampus through its ventral subregion. Journal of Neuroscience, 33(35), 14211-14224.

Oishi, Y., & Lazarus, M. (2017). The control of sleep and wakefulness by mesolimbic dopamine systems. Neuroscience research, 118, 66-73.

Perreault, M. L., Fan, T., Banasikowski, T. J., Grace, A. A., & George, S. R. (2017). The atypical dopamine receptor agonist SKF 83959 enhances hippocampal and prefrontal cortical neuronal network activity in a rat model of cognitive dysfunction. European Journal of Neuroscience, 46(4), 2015-2025.

Phillips, A. G., Ahn, S., & Floresco, S. B. (2004). Magnitude of dopamine release in medial prefrontal cortex predicts accuracy of memory on a delayed response task. Journal of Neuroscience, 24(2), 547-553.

Ruggiero, R. N., Rossignoli, M. T., Marques, D. B., de Sousa, B. M., Romcy-Pereira, R. N., Lopes-Aguiar, C., & Leite, J. P. (2021). Neuromodulation of hippocampal-prefrontal cortical synaptic plasticity and functional connectivity: implications for neuropsychiatric disorders. Frontiers in cellular neuroscience, 15.

Schall, K. P., & Dickson, C. T. (2010). Changes in hippocampal excitatory synaptic transmission during cholinergically induced theta and slow oscillation states. Hippocampus, 20(2), 279-292.

Schneider, M., Broggini, A. C., Dann, B., Tzanou, A., Uran, C., Sheshadri, S., ... & Vinck, M. (2021). A mechanism for inter-areal coherence through communication based on connectivity and oscillatory power. Neuron, 109(24), 4050-4067.

Siapas, A. G., Lubenov, E. V., & Wilson, M. A. (2005). Prefrontal phase locking to hippocampal theta oscillations. Neuron, 46(1), 141-151.

Sigurdsson, T., Stark, K. L., Karayiorgou, M., Gogos, J. A., & Gordon, J. A. (2010). Impaired hippocampal–prefrontal synchrony in a genetic mouse model of schizophrenia. Nature, 464(7289), 763-767.

Sigurdsson, T., & Duvarci, S. (2016). Hippocampal-prefrontal interactions in cognition, behavior and psychiatric disease. Frontiers in systems neuroscience, 9, 190.

Sirota, A., Montgomery, S., Fujisawa, S., Isomura, Y., Zugaro, M., & Buzsáki, G. (2008). Entrainment of neocortical neurons and gamma oscillations by the hippocampal theta rhythm. Neuron, 60(4), 683-697.

Skirboll, L. R., Grace, A. A., & Bunney, B. S. (1979). Dopamine auto-and postsynaptic receptors: electrophysiological evidence for differential sensitivity to dopamine agonists. Science, 206(4414), 80-82.

Spellman, T., Rigotti, M., Ahmari, S. E., Fusi, S., Gogos, J. A., & Gordon, J. A. (2015). Hippocampal–prefrontal input supports spatial encoding in working memory. Nature, 522(7556), 309-314.

Uhlhaas, P. J., Roux, F., Rodriguez, E., Rotarska-Jagiela, A., & Singer, W. (2010). Neural synchrony and the development of cortical networks. Trends in cognitive sciences, 14(2), 72-80.

Varela, F., Lachaux, J. P., Rodriguez, E., & Martinerie, J. (2001). The brainweb: phase synchronization and large-scale integration. Nature reviews neuroscience, 2(4), 229-239.

Vinck, M., Oostenveld, R., Van Wingerden, M., Battaglia, F., & Pennartz, C. M. (2011). An improved index of phase-synchronization for electrophysiological data in the presence of volume-conduction, noise and sample-size bias. Neuroimage, 55(4), 1548-1565.

Vinck, M., van Wingerden, M., Womelsdorf, T., Fries, P., & Pennartz, C. M. (2010). The pairwise phase consistency: a bias-free measure of rhythmic neuronal synchronization. Neuroimage, 51(1), 112-122.

Yanagihashi, R., Yamanouchi, K., & Ishikawa, T. (1991). The effects of apomorphine on the hippocampal field potential in freely moving rats: pharmacological evidence of the involvement of D2 receptors. Neuropharmacology, 30(2), 177-182.

Xu, D., Karain, B., Brantley, E., & Shi, W. X. (2011). Effects of L-DOPA on nigral dopamine neurons and local field potential: comparison with apomorphine and muscimol. Journal of Pharmacology and Experimental Therapeutics, 337(2), 533-539.

Xu, X., Zheng, C., An, L., Wang, R., & Zhang, T. (2016). Effects of dopamine and serotonin systems on modulating neural oscillations in hippocampus-prefrontal cortex pathway in rats. Brain topography, 29(4), 539-551.

Figures and Legends

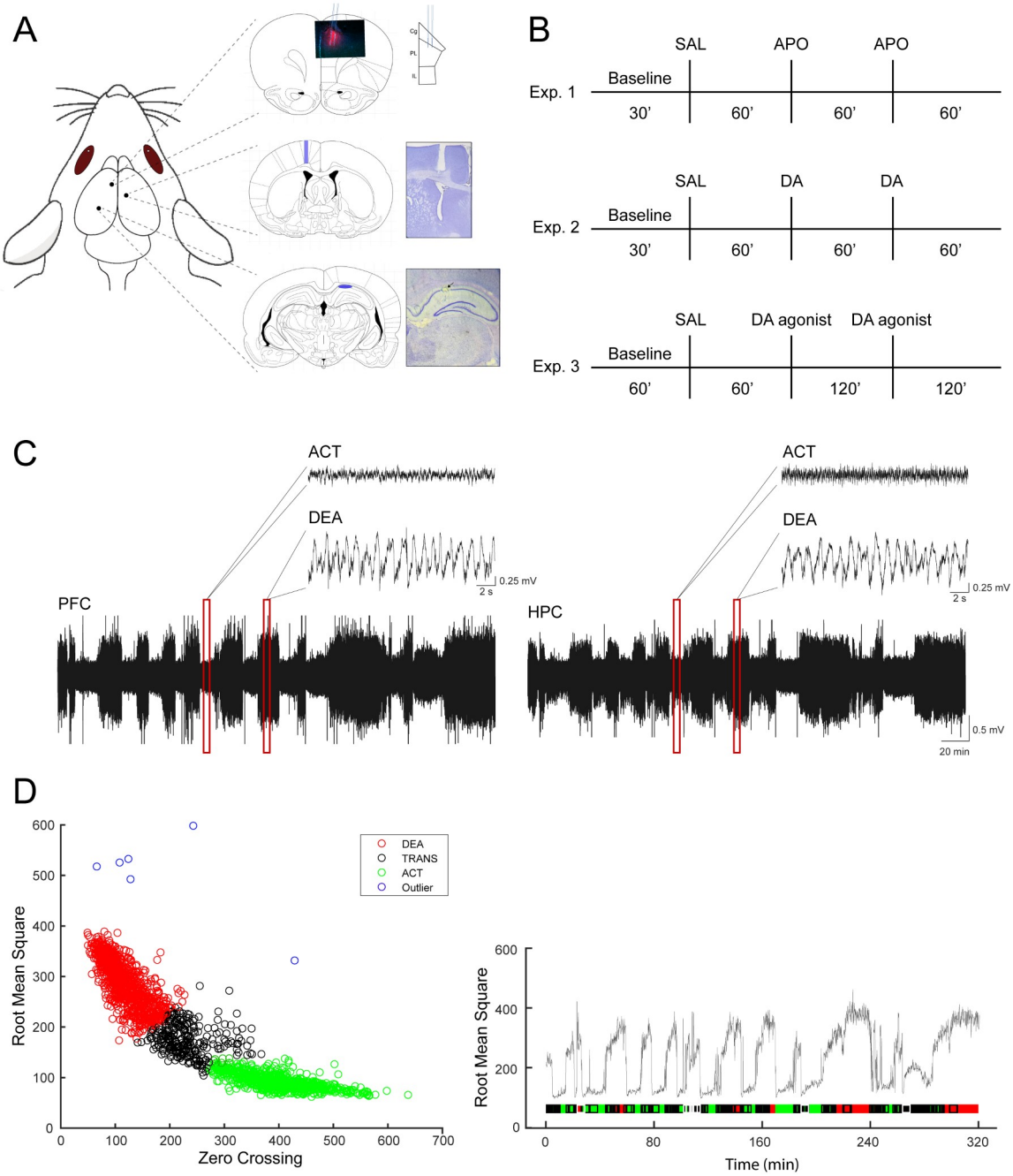

Figure 1. Experimental procedures and classification of oscillatory states under urethane anesthesia. (**A**). Histological sections showing the positioning of the cannula for i.c.v. drug injection e of the electrodes and the silicon probe for recording neural activity. (**B**) Experimental design. (**C**) Representative 320 min recording of raw LFP (bottom) and magnification of 20-second segments showing the spontaneous oscillatory pattern of ACT and DEA states in PFC and HPC (top). (**D**) Classification of oscillatory states under urethane anesthesia. Initially, the states were clustered in an unsupervised manner into three groups by the k-means algorithm. Then, manual adjustments were made to refine the classification. Grouping of 10-second epochs into three categories based on root mean square (RMS) and zero crossings. Epochs with high deviation from the cluster's mean were considered outliers and removed from the analyses. Comparison of each epoch RMS value with its respective classification.

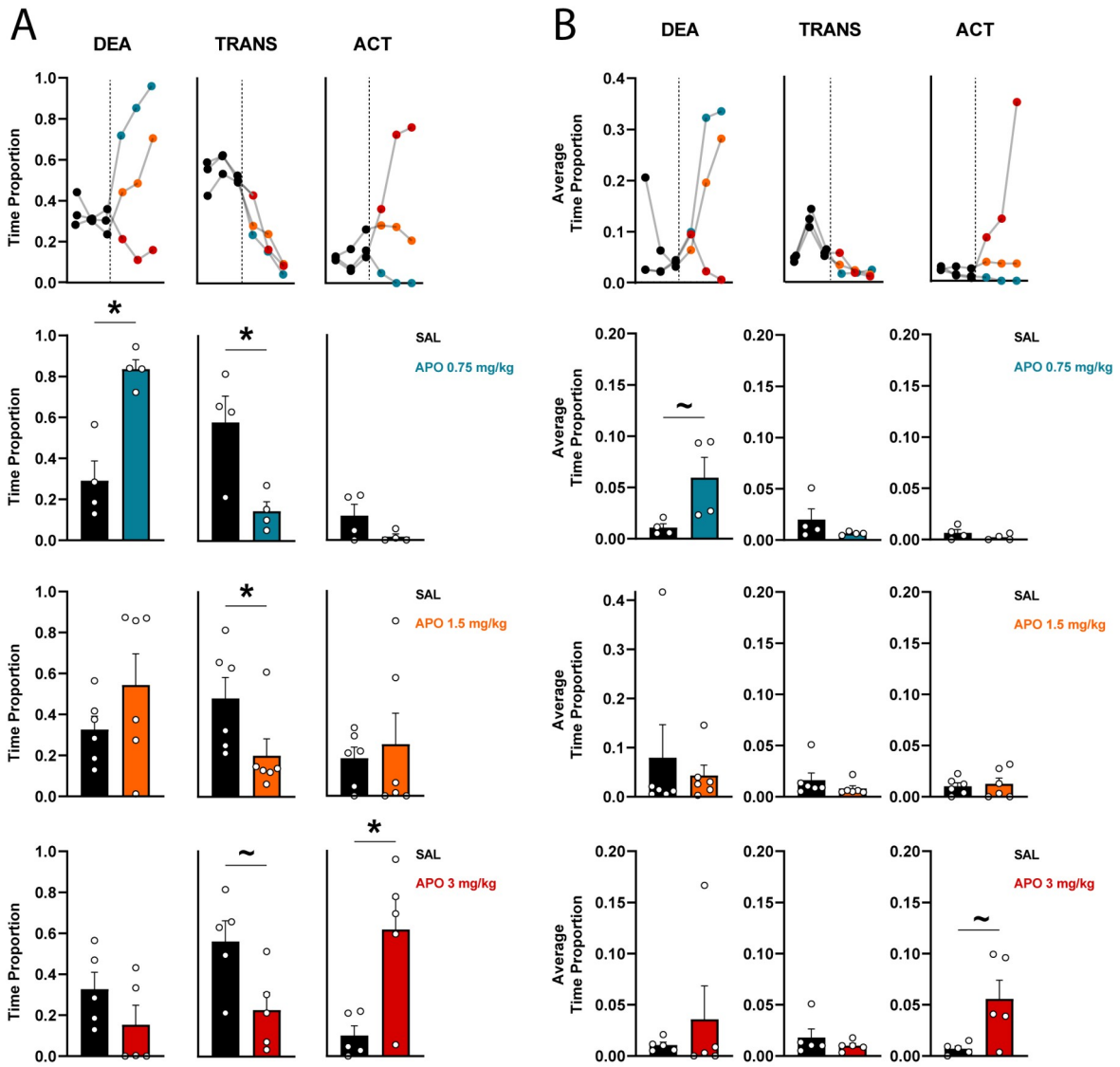

Figure 2. Apomorphine exhibits a dose-dependent effect on the time proportion of oscillatory states. (**A-B**), Line graphs represent the time proportion of states over time, where each point corresponds to an 18-minute block. The dotted vertical line represents the drug injection. The bar graphs correspond to the mean of the blocks of each treatment. (**A**) The proportion of time is obtained by summing the total time during which the respective state occurs. We observed that all doses induce a reduction in the time proportion of TRANS states, which indicates expressive oscillatory shifting to DEA or ACT states. Furthermore, while the 0.75 mg/kg dose induced a significant increase in time proportion of DEA states, the 3 mg/kg dose induced a significant increase in time proportion of ACT states. (**B**) The average time proportion is obtained by averaging the total time during which the respective state occurs. This measure indicates whether a change in the duration of a state is consistent across occurrences of the respective state. We observed that the 0.75 mg/kg dose increases the average time proportion in DEA states, while the 3 mg/kg dose increases in ACT states. Data presented as mean ± SEM. ~p<0.1, *p<0.05.

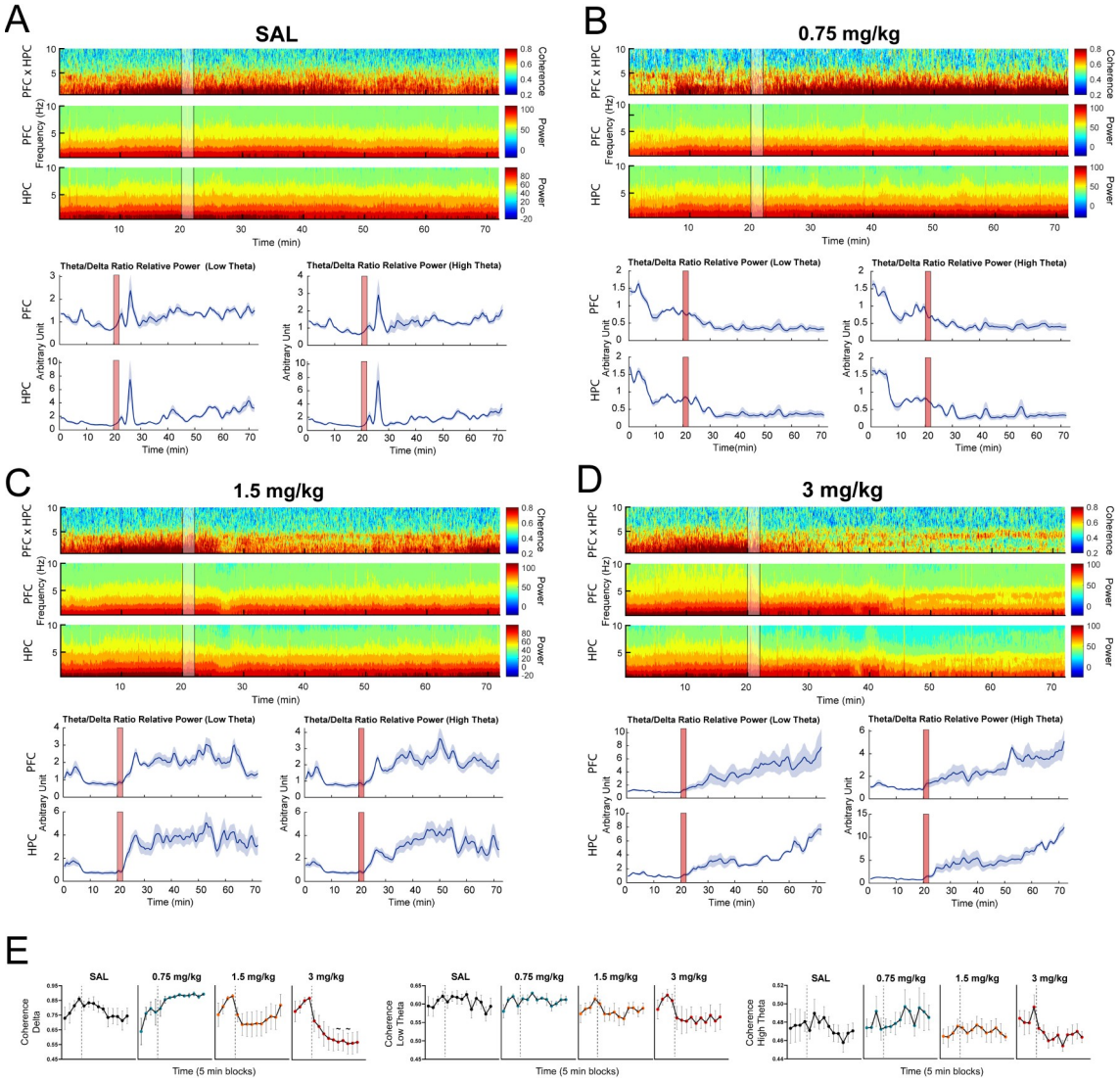

Figure 3. Effects of Apomorphine administration on HPC-PFC dynamics (**A-D**) HPC-PFC coherence and power spectrograms, respectively, for saline injection and three doses of apomorphine. Below the spectrograms, graphs display the relative power of the theta/delta ratio considering two different frequency ranges in the theta band. Theta/delta ratio data are normalized by baseline. Vertical rectangles on spectrograms and theta/delta ratio plots represent the injection period (2 minutes duration). We observed a dose-dependent effect of apomorphine on theta/delta ratio. The 0.75 mg/kg dose reduces the theta/delta ratio (**B**), while 1.5 mg/kg and 3 mg/kg doses increase (**C-D**). (**E**) HPC-PFC coherence over time quantified in 5-minutes blocks for each frequency band. The first four points of the line graphs correspond to the baseline (total period of 20 minutes), and the remaining points correspond to the post-injection period (total period of 54 minutes). Post-injection blocks were compared with the mean of baseline blocks. Data presented as mean ± SEM. ~p<0.1.

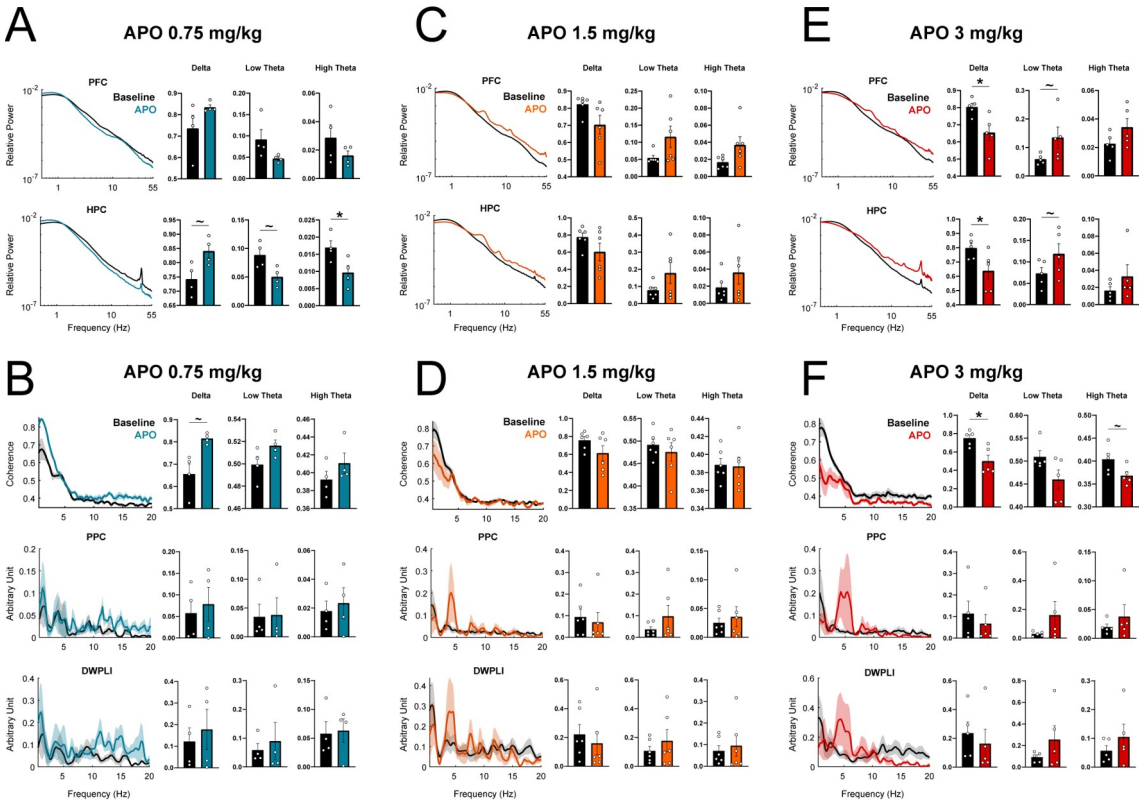

Figure 4. Apomorphine exhibits a dose-dependent effect on HPC-PFC connectivity. Statistical comparisons between the 30-40 minutes period mean after apomorphine injection and the respective injection averaged baseline. (**A-C**) PFC and HPC averaged PSDs. (**D-F**) HPC-PFC synchrony is represented by measures of coherence (top), pairwise phase consistency (PPC, middle), and debiased weighted phase lag index (DWPLI, bottom). Apomorphine 0.75 mg/kg dose increases relative power (HPC) and coherence (HPC-PFC) in delta (**A, D**) and decreases relative power (HPC) in theta frequencies (**A**). In contrast, the 3 mg/kg dose decreases relative power in delta and increases in high theta in both regions (**C**), as well as reduces HPC-PFC coherence in delta and high theta (**F**). The 1.5 mg/kg dose increases theta oscillations in PSDs (**B**), and similarly to the 3mg/kg dose, it shows PPC and DWPLI peaks in theta frequencies (**E, F**), but there are no statistical differences. Data presented as mean ± SEM. ~p<0.1, *p<0.05.

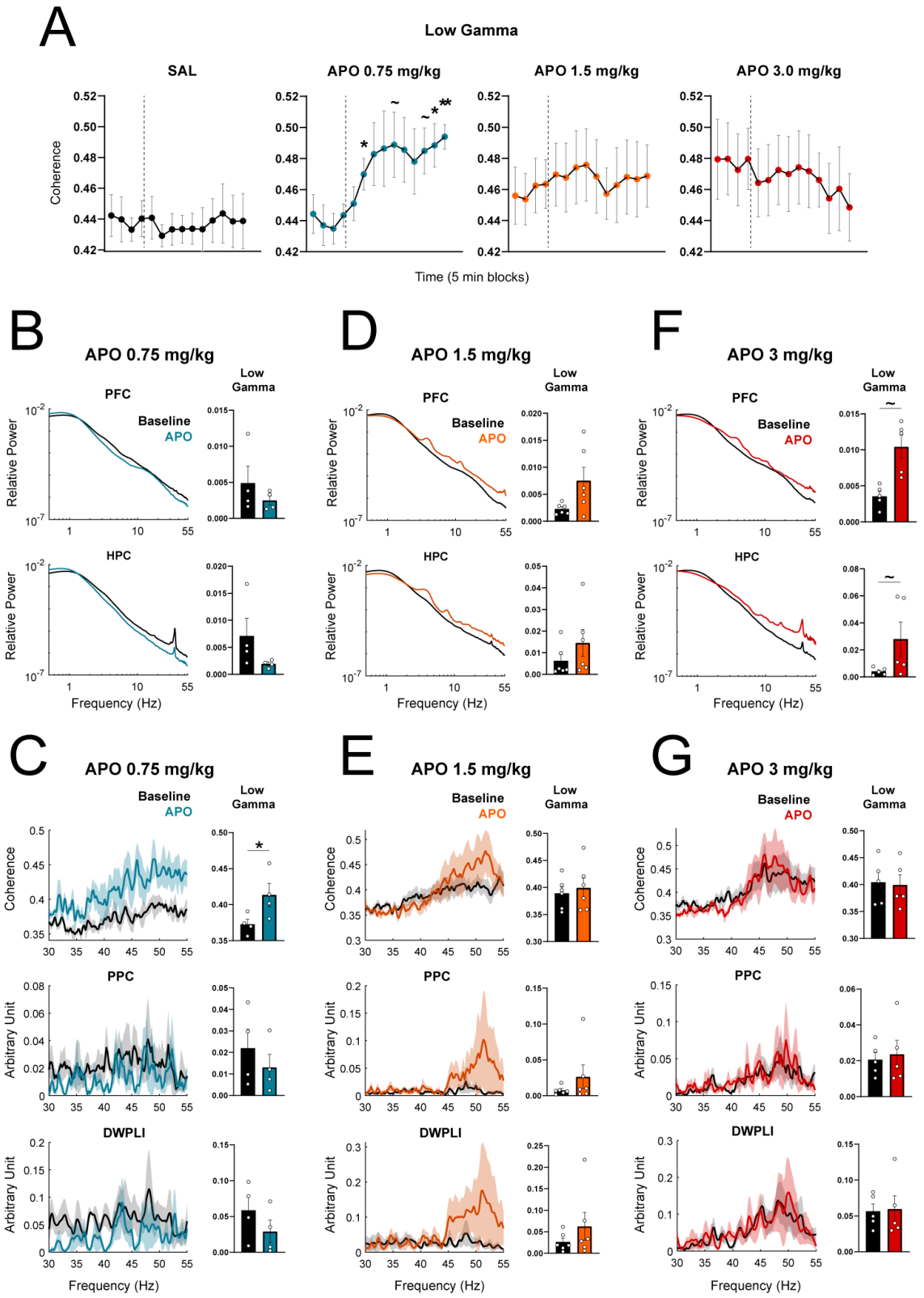

Figure 5. Apomorphine exhibits a dose-dependent effect on HPC-PFC gamma connectivity. Statistical comparisons between the 30-40 minutes period mean after apomorphine injection and the respective injection averaged baseline at 30-55Hz gamma band frequencies. (**A**) HPC-PFC low gamma coherence over time quantified in 5-minute blocks. A continuous increase in coherence is noted over time after the 0.75 mg/kg APO dose injection, which is not observed at the other doses administered. (**B-D**) PFC and HPC averaged PSDs. (**E-G**) HPC-PFC synchrony is

represented by measures of coherence (top), pairwise phase consistency (PPC, middle), and debiased weighted phase lag index (DWPLI, bottom). Data presented as mean ± SEM. ~p<0.1, *p<0.05. The observed effects were an increase in HPC-PFC coherence with no change in relative power after 0.75 mg/kg APO dose injection (**B, E**) and an increase in relative power after APO 3 mg/kg dose injection with no change in HPC-PFC synchrony (**D, G**). No statistical effect was observed after APO 1.5 mg/kg injection (**C, F**).

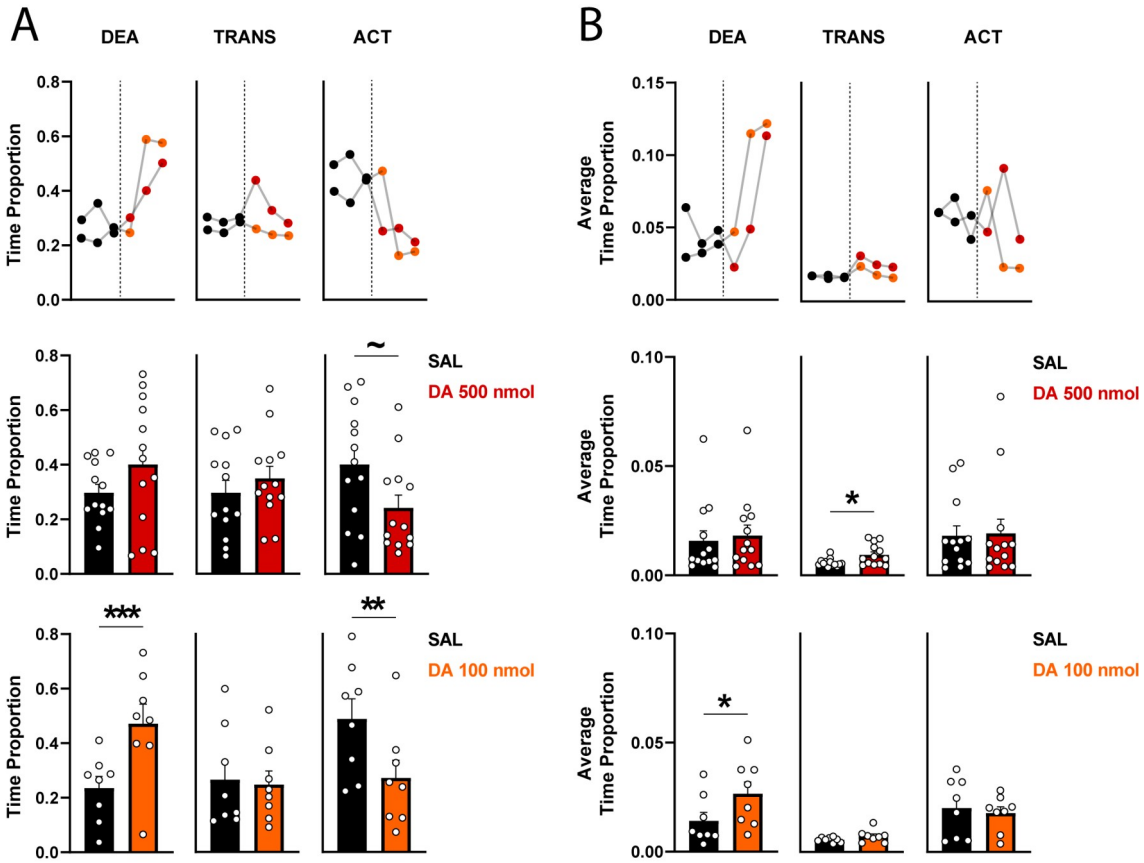

Figure 6. Dopamine affects the duration of oscillatory states in a dose-dependent manner. (**A-B**) Line graphs displaying time proportion (left-top) or average time proportion (right-top) of states in saline or dopamine injections (100 nmol and 500 nmol doses). The bar graphs correspond to the mean of the blocks of each treatment. We observed that DA 100 nmol induces the prevalence of DEA states. (A) DA 100 nmol increases the time proportion in DEA states while it decreases in ACT states. (B) DA 100 nmol also reduces the average time proportion in ACT states, while DA 500 nmol increases in TRANS states.. Data presented as mean ± SEM. ~p<0.1, *p<0.05, **p<0.01, ***p<0.001.

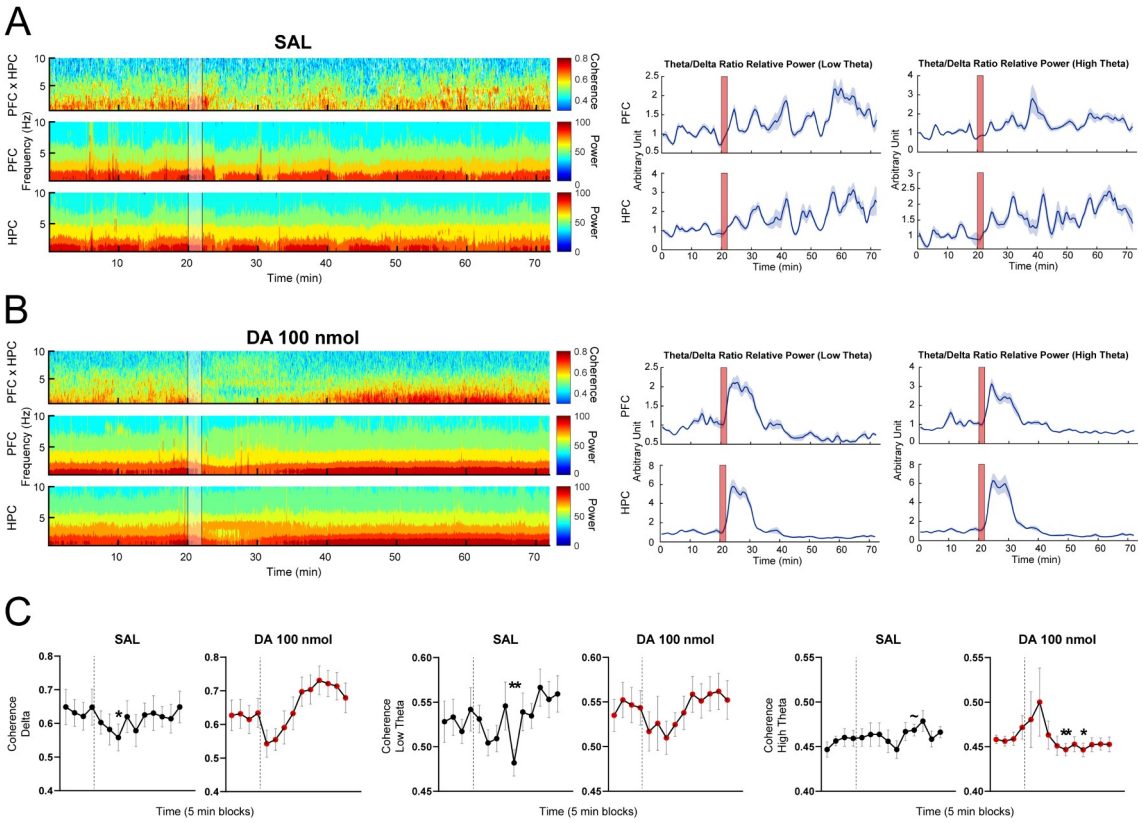

Figure 7. Effects of 100 nmol Dopamine administration on HPC-PFC dynamics. (**A-B**) HPC-PFC coherence and power spectrograms, respectively, for saline injection and dopamine 100 nmol dose. Below the spectrograms, graphs display the relative power of the theta/delta ratio considering two different frequency ranges in the theta band. Theta/delta ratio data are normalized by baseline. Vertical rectangles on spectrograms and theta/delta ratio plots represent the injection period (2 minutes duration). (**B**) DA 100 nmol increases HPC-PFC theta coherence and relative power of theta/delta ratio for at least 10 minutes after injection. The theta/delta ratio returns to baseline levels over the next 40 minutes, indicating delta power predominance and suggesting a reduction in state switching. Note that after saline injection (**A**), the line on the theta/delta ratio graph has many peaks and valleys, reflecting changes in power generated by spontaneous switching between oscillatory states of anesthesia. (**C**) HPC-PFC coherence over time was quantified in 5-minutes blocks for each frequency band. Data presented as mean ± SEM. ~p<0.1, *p<0.05, **p<0.01.

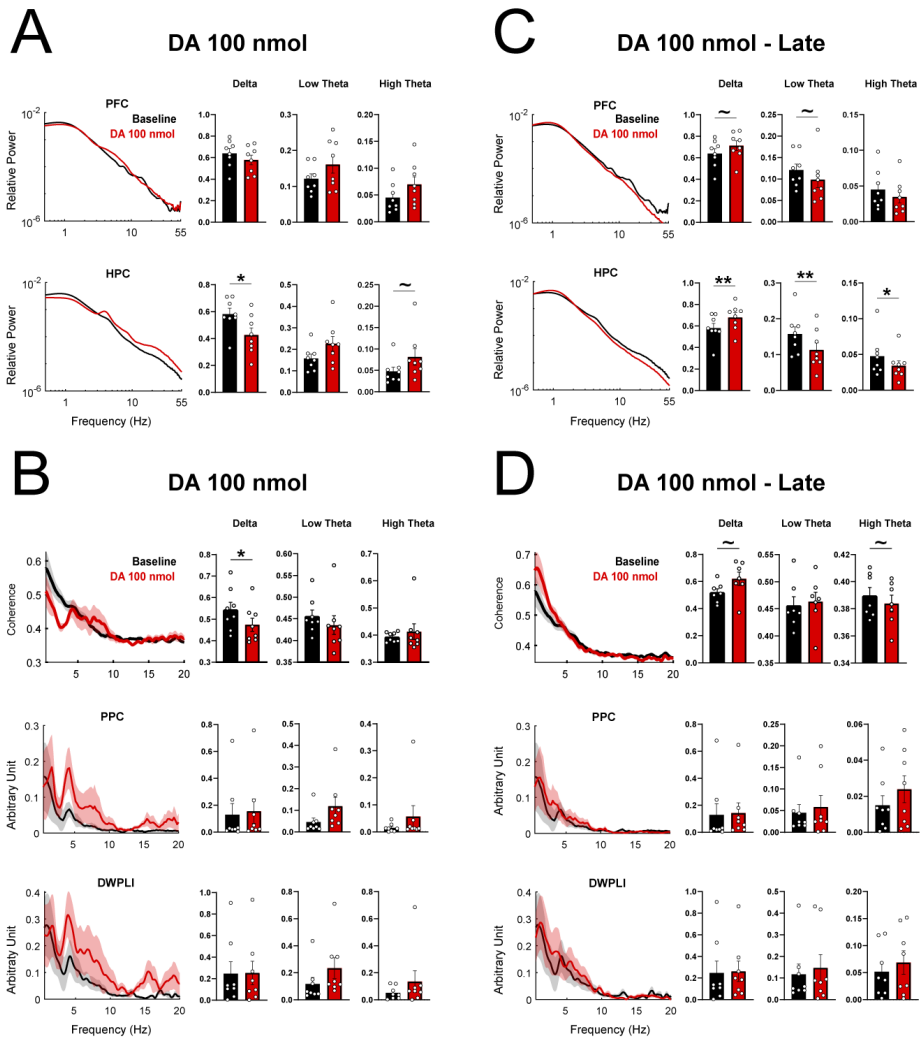

Figure 8. Dopamine 100 nmol changes HPC-PFC connectivity. Statistical comparisons between averaged periods after injection (**A**, **C**, initial period, 2-12 minutes after injection; **B**, **D**, late period, 30-40 minutes after injection) and the respective injection averaged baseline. (**A-B**) PFC and HPC averaged PSDs. (**C-D**) HPC-PFC synchrony is represented by measures of coherence (top), pairwise phase consistency (PPC, middle), and debiased weighted phase lag index (DWPLI, bottom). (**A, C**) In the initial period, DA 100 nmol decreases delta relative power (HPC) and coherence (HPC-PFC), and increases high theta relative power (HPC). (**B, D**) In the late period, DA 100 nmol increases delta relative power and coherence (HPC-PFC), and decreases low theta (HPC and PFC) and high theta (HPC) relative power. Data presented as mean ± SEM. ~p<0.1, *p<0.05.

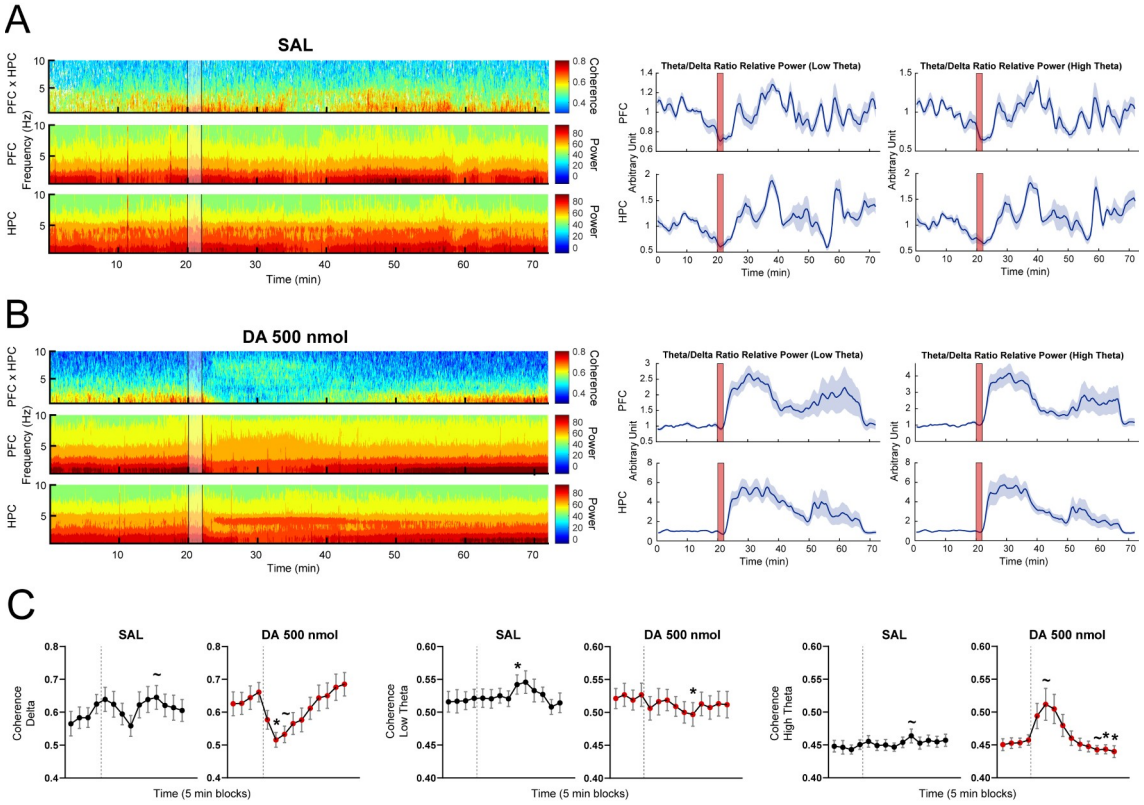

Figure 9. Effects of 500 nmol Dopamine administration on HPC-PFC dynamics. (**A-B**) HPC-PFC coherence and power spectrograms, respectively, for saline injection and dopamine 500 nmol dose. Below the spectrograms, graphs display the relative power of the theta/delta ratio considering two different frequency ranges in the theta band. Theta/delta ratio data are normalized by baseline. Vertical rectangles on spectrograms and theta/delta ratio plots represent the injection period (2 minutes duration). (**B**) DA 500 nmol increases coherence in theta frequencies and relative power of theta/delta ratio for approximately 20 minutes after injection. The theta/delta ratio does not return to baseline levels for the next 30 minutes, indicating a prolonged effect of DA gradually dissipating over time. (**C**) HPC-PFC spectral coherence over time was quantified in 5-minutes blocks for each frequency band. Data presented as mean ± SEM. ~p<0.1, *p<0.05.

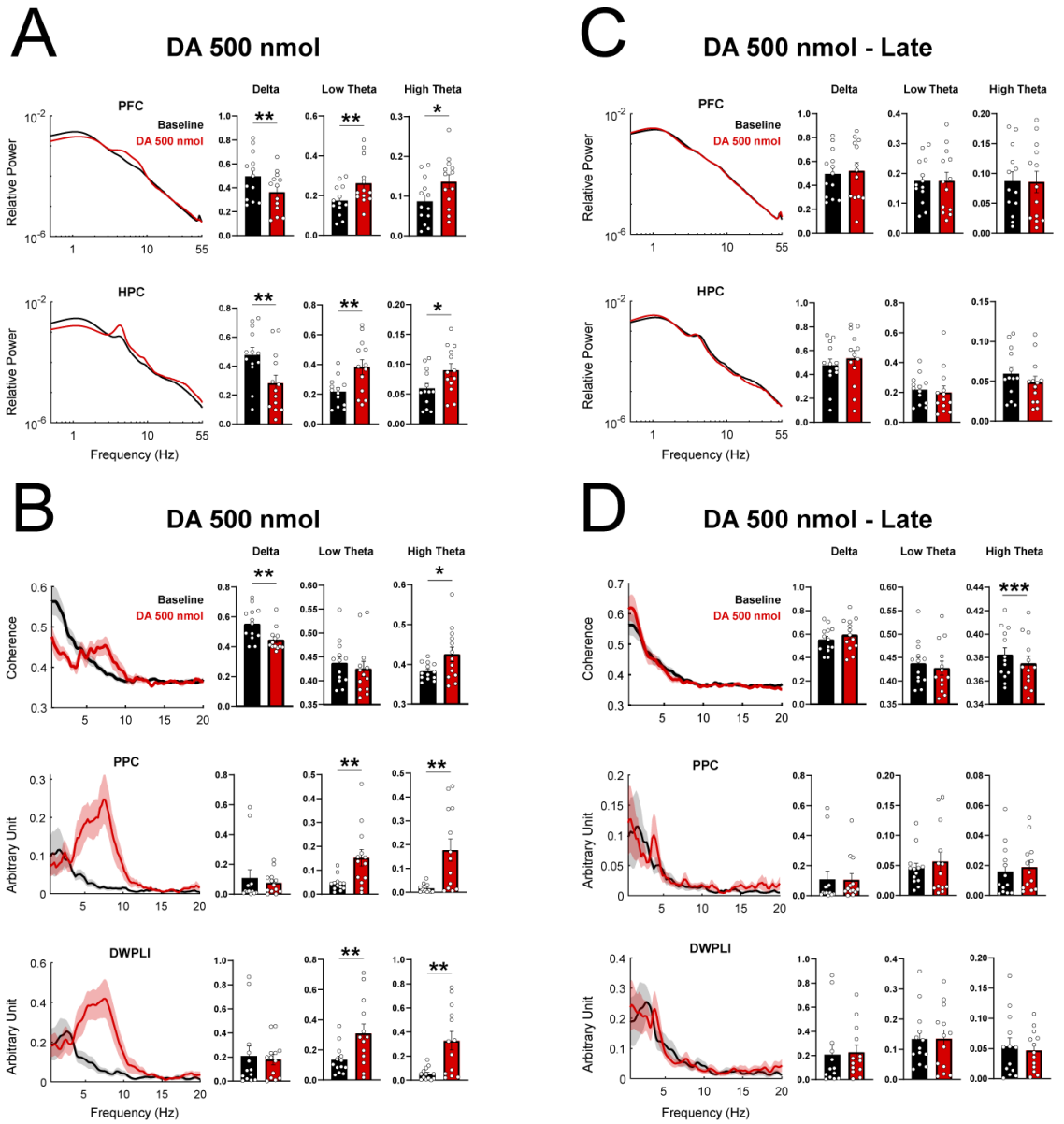

Figure 10. Dopamine 500 nmol changes HPC-PFC connectivity. Statistical comparisons between averaged periods after injection (**A**, **C**, initial period, 2-12 minutes after injection; **B**, **D**, late period, 30-40 minutes after injection) and the respective injection averaged baseline. (**A-B**) PFC and HPC averaged PSDs. (**C-D**) HPC-PFC synchrony is represented by measures of coherence (top), pairwise phase consistency (PPC, middle), and debiased weighted phase lag index (DWPLI, bottom). (**A, C**) In the initial period, DA 500 nmol induces a general increase in relative power and synchrony (HPC-PFC) in theta frequencies, except for low theta coherence (HPC-PFC). Note also the reduction in delta relative power and coherence (HPC-PFC). (**B, D**) In the late period, DA 500 nmol reduces high theta coherence (HPC-PFC) but does not change other measures. Data presented as mean ± SEM. *p<0.05, **p<0.01, ***p<0.005.

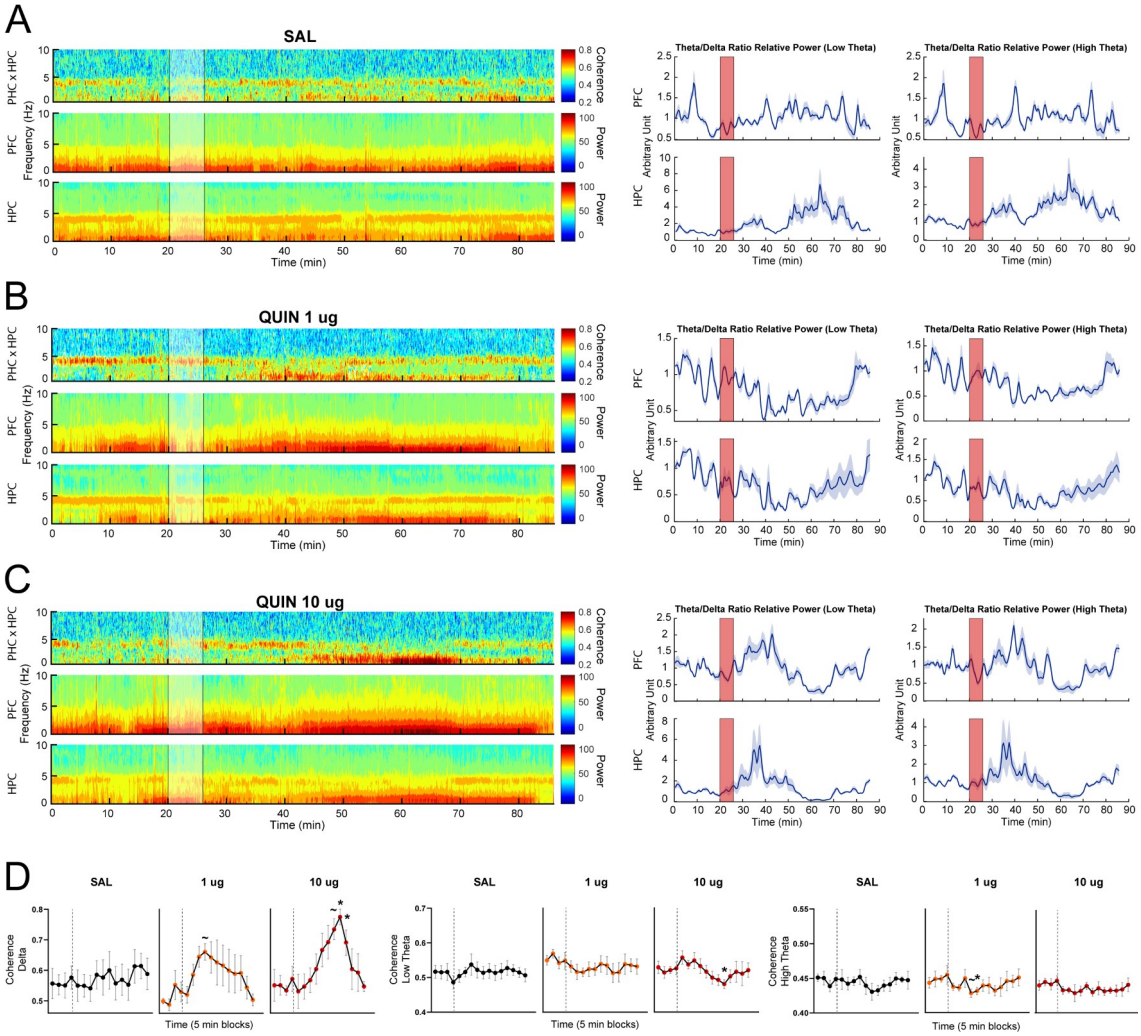

Figure 11. Quinpirole effects on HPC-PFC dynamics. (**A-C**) HPC-PFC coherence and power spectrograms, respectively, for saline injection and QUIN doses (1 µg and 10 µg). Below the spectrograms, the graphs display the relative power of the theta/delta ratio considering two different frequency ranges in the theta band. Theta/delta ratio data are normalized by baseline. Vertical rectangles on spectrograms and theta/delta ratio plots represent the injection period (6 minutes duration). (**D**) HPC-PFC spectral coherence over time was quantified in 5-minutes blocks for each frequency band. (**B, D**) QUIN 1 µg produces no significant changes in the relative power of the theta/delta ratio relative to saline injection but increases coherence peaking 20 minutes after injection. (**C, D**) QUIN 10 µg induces a transient increase in the relative power of the theta/delta ratio in the first 20 minutes and a progressive increase in delta coherence, whose peak occurs between 35 and 45 minutes after injection. Data presented as mean ± SEM. ~p<0.1, *p<0.05.

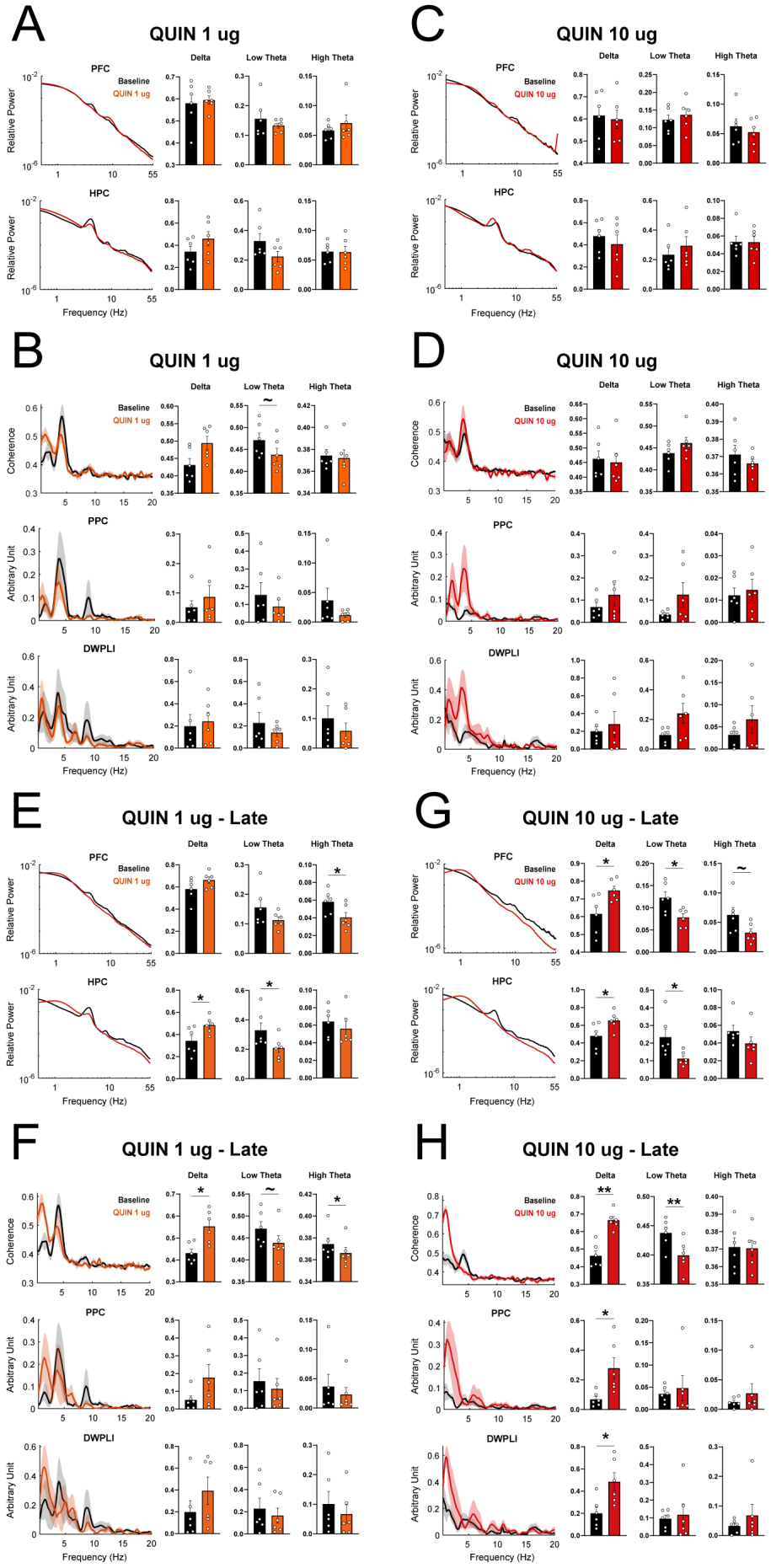
A
QUIN 1 ug
PFC
HPC
Baseline
QUIN 1 ug
Relative Power
Frequency (Hz)
Delta
Low Theta
High Theta
B
QUIN 1 ug
Coherence
PPC
DWPLI
Arbitrary Unit
C
QUIN 10 ug
QUIN 10 ug
D
QUIN 10 ug
E
QUIN 1 ug - Late
F
QUIN 1 ug - Late
G
QUIN 10 ug - Late
H
QUIN 10 ug - Late

Figure 12. Quinpirole changes HPC-PFC connectivity. Statistical comparisons between averaged periods after injection (**A-D**, initial period, 2-12 minutes after injection; E-H, late period, 30-40 minutes after injection) and the respective injection averaged baseline. (**A, B, E, F**) PFC and HPC averaged PSDs. (**C, D, G, H**) HPC-PFC synchrony is represented by measures of coherence (top), pairwise phase consistency (PPC, middle), and debiased weighted phase delay index (DWPLI, bottom). (**A, C**) In the initial period, QUIN 1 µg decreases HPC-PFC low theta coherence but does not change the other measures. (**B, D**). QUIN 10 µg did not significantly affect HPC-PFC power and synchrony. (**E-H**) The main effects of QUIN occur in the late period. (**E, F**) Both doses induce a late increase in relative power in delta (QUIN 1 µg, HPC; QUIN 10 µg, HPC and PFC) and a decrease in theta frequencies (QUIN 1 µg, theta 6-10Hz in PFC, theta 3-6 Hz in HPC; QUIN 10 µg, theta 3-10 Hz in PFC, theta 3-6 Hz in HPC). (**G, H**) There is also an increase in delta synchrony (QUIN 1 µg, coherence; QUIN 10 µg, coherence, PPC, and DWPLI) and a reduction in theta synchrony (QUIN 1 µg, coherence, theta 3- 10 Hz; QUIN 10 µg, coherence, theta 3-6 Hz). Data presented as mean ± SEM. ~$p<0.1$, *$p<0.05$.